

Online Appendix A: Important Properties of the SML Estimator

[Kristensen and Shin \(2012\)](#) argue that the main advantage of the SML is its general applicability. Starting with observables, the density estimator based on i.i.d. draws is not affected by potential dependence structures in the data, and the SML works even if the observables z_t are non-stationary. An important issue to consider is a potential curse of dimensionality with respect to the dimension of the vector of observables, as we smooth only over z_t . Generally, for multi-dimensional models, the estimation performance deteriorates as $l \equiv \dim(z_t)$ increases. We devote careful attention to this issue and extensively study the estimation performance of the SML for the three-equation NKM in [Section 5](#). Importantly, the SML does not suffer from the usual curse of dimensionality associated with kernel estimators, as substantially discussed in [Kristensen and Shin \(2012\)](#). The variance component of the resulting estimator does not need to be controlled by an unbearably large number of simulations, as the summation in equation (17) reveals an additional smoothing effect and the additional variance of $\hat{L}_T(\theta)$ caused by simulations recovers the standard parametric rate of $1/N$. Hence, the curse of dimensionality remains only of order $l \equiv \dim(z_t)$, and the SML will behave similarly to other estimation techniques including MLE in this respect.

On the other hand, given the kernel approximation method and its asymptotic properties, the simulated $\hat{L}_T(\theta)$ is generally a biased estimator of the actual $L_T(\theta)$ for a fixed approximation precision N and bandwidth $H > \mathbf{0}$. Only $N \rightarrow \infty$ and $H \rightarrow \mathbf{0}$ imply asymptotic consistency. Careful attention thus needs to be devoted to the selection of the bandwidth H with respect to a simulation size and a specific sample of data. Fortunately, in a simulation study, [Kristensen and Shin \(2012\)](#) demonstrate that the SML performs well using a broad range of bandwidths. A standard identification assumption for the stationary case requires $\mathbb{E}[\log p(z_t|x_t, \theta)] < \mathbb{E}[\log p(z_t|x_t, \theta_0)]$, $\forall \theta \neq \theta_0$. [Altissimo and Mele \(2009\)](#) argue that under its stronger version, the specific choice of bandwidth H is even less important because one can prove the consistency for any fixed $\mathbf{0} < H < \bar{H}$ for some

\bar{H} as $N \rightarrow \infty$. This suggests that the proposed methodology is robust to the choice of H from a theoretical perspective because one can assuredly well identify model parameters in large finite samples after \bar{H} is set. However, in a practical application, one still needs to know the threshold level of \bar{H} that can be examined through simulations. In addition to a proper selection of N and H , the kernel K itself is assumed to satisfy conditions K.1–2 specified in [Kristensen and Shin \(2012, pg. 81\)](#), i.e., to be continuously differentiable, allow for unbounded support, and belong to so-called higher-(than second)-order or bias-reducing kernels. For instance, from the most commonly used kernels the Gaussian kernel naturally satisfies all given assumptions. Higher number of derivatives of p then facilitate a faster rate of convergence and determine the degree of bias reduction for the estimated conditional density \hat{p} .

With respect to additional theoretical properties, [Kristensen and Shin \(2012\)](#) demonstrate that the SML $\hat{\theta}$ is first-order asymptotically equivalent to the infeasible MLE $\tilde{\theta}$ under a set of general conditions satisfied by most models and ensuring that $\hat{p} \rightarrow p$ sufficiently fast, allowing even for mixed discrete and continuous distributions and non-stationarity of the dependent variables. A set of regularity conditions (A.1–4, K.1–2, pg. 80–81) on the model and its associated conditional density is defined to satisfy these general conditions for uniform convergence rates of kernel estimators stated in [Kristensen \(2009\)](#). Moreover, under additional assumptions including, e.g., stationarity, results regarding the higher-order asymptotic properties together with expressions for the bias and variance components of the SML estimator (compared to the actual MLE) due to kernel estimation and numerical simulations are derived.

Online Appendix B: Memory Parameter

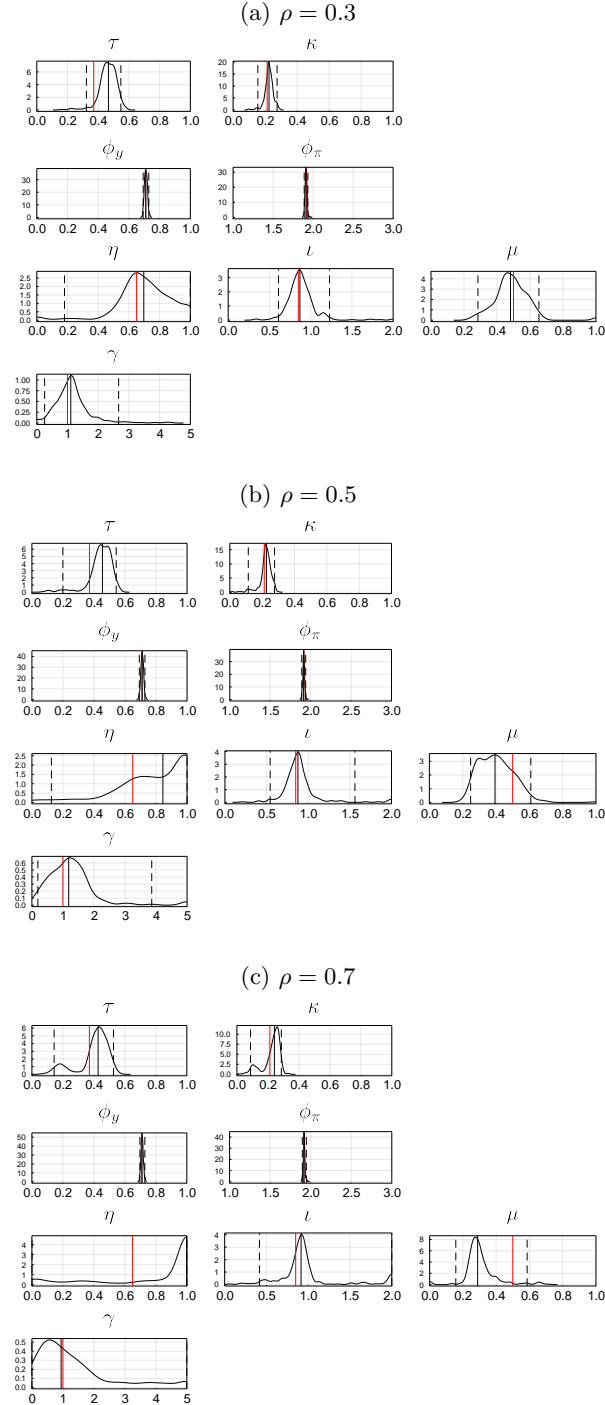


Figure 7: Densities of the pseudo-true parameter estimates for an alternative BR NKM with a non-zero memory parameter ρ . Bold black curves depict kernel density estimates of the sample densities, bold red vertical lines show the pseudo-true values, and dashed red vertical lines depict 95% confidence intervals of the sample estimates. Based on 300 random runs, $T = 500$, the parametrization follows [Table 1](#).

Online Appendix C: Comparison to the Simulated Method of Moments

Table 4: Estimates for the BR NKM via the SMM

	Par.	BR forward-looking NKM		
		$T=250$	500	5000
τ	<i>.371</i>	.38	.37	.38
$\langle 0, 1 \rangle$		(.26-.50)	(.29-.47)	(.32-.44)
κ	<i>.213</i>	.21	.22	.21
$\langle 0, 1 \rangle$		(.14-.32)	(.16-.30)	(.17-.29)
ϕ_y	<i>.709</i>	.70	.71	.71
$\langle 0, 1 \rangle$		(.52-.94)	(.56-.90)	(.55-.87)
ϕ_π	<i>1.914</i>	1.94	1.95	1.97
$\langle 1, 3 \rangle$		(1.65-2.25)	(1.73-2.17)	(1.77-2.20)
η	<i>.65</i>	.72	.77	.62
$\langle 0, 1 \rangle$		(.02-.99)	(.01-.99)	(.07-.98)
ι	<i>.85</i>	.69	.64	.70
$\langle 0, 2 \rangle$		(.13-1.23)	(.16-1.08)	(.28-1.08)
μ	<i>.50</i>	.54	.51	.54
$\langle 0, 1 \rangle$		(.23-.79)	(.27-.74)	(.40-.68)
γ	<i>1.00</i>	1.96	2.05	2.13
$\langle 0, 5 \rangle$		(.04-4.72)	(.05-4.70)	(.08-4.64)

Constraints for optimization and its starting point are given in $\langle \rangle$ brackets. T denotes the length of the executed time series. Sample medians based on 300 random runs are reported while the 95% confidence intervals of the sample estimates are reported in $()$ parentheses. The parametrization follows [Table 1](#). Figures are rounded to 2 or 3 decimal places. The SMM setup follows [Jang and Sacht \(2016, 2019\)](#); [Franke \(2019\)](#). The reported results are directly comparable to [Table 1](#), left half.

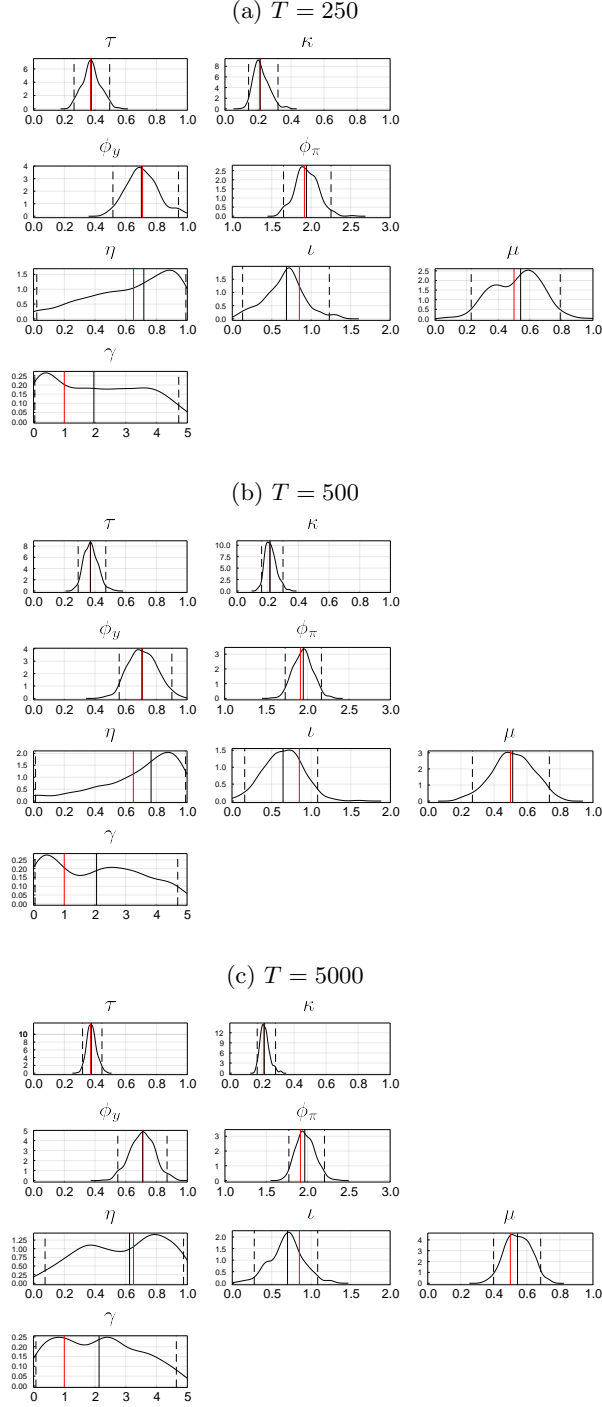


Figure 8: Densities of the pseudo-true parameter estimates for the BR NKM via the SMM following the setup by [Jang and Sacht \(2016, 2019\)](#); [Franke \(2019\)](#). Bold black curves depict kernel density estimates of the sample densities, bold red vertical lines show the pseudo-true values, and dashed red vertical lines depict 95% confidence intervals of the sample estimates. Based on 300 random runs, the parametrization follows [Table 1](#). The reported results are directly comparable to [Figure 1](#), left half.